International Summer Institute for Modeling in Astrophysics

ISIMA Report on The Effect of Mass Segregation and Metallicity on Mass-to-Light Ratio Measurements of Globular Clusters

Author:
Rosemary Shanahan[1]

Supervisors:
Prof. Mark Gieles[2]
Dr. Anna Lisa Varri[3]

Abstract

In this work, we develop parameterised models for the present day mass function of globular clusters that includes the effects of stellar evolution and dynamics. Predictions from these models are compared with the observational data of globular clusters in M31 in an attempt to explain the discrepancy between observed mass-to-light ratios and those predicted from a Kroupa IMF model. We found that the amount of remnants within the globular clusters dramatically alters the measured dynamical mass compared to the actual mass and that this could go some way to explaining the observed discrepancy.

[1]Institute for Astronomy, University of Edinburgh, Royal Observatory, Blackford Hill, Edinburgh EH9 3HJ, UK.
[2]Department of Physics, University of Surrey, Guildford, GU2 7XH, UK.
[3]School of Mathematics and Maxwell Institute for Mathematical Sciences, University of Edinburgh, Edinburgh EH9 3JZ, UK.

Contents

1 Introduction

1.1 Background

The initial mass function (IMF) is defined as the number of stars per unit volume per unit logarithmic mass; it describes the distribution of initial masses of a stellar population. One of the most discussed yet unanswered questions in astrophysics is whether or not the IMF is universal. This question is important because the initial mass of a star dictates its subsequent evolutionary path and therefore the IMF influences most of the observable properties of stellar populations and galaxies. Establishing whether or not there are variations in the IMF could provide insights into the stellar formation processes.

1.2 Measuring the IMF

A common way to measure the IMF is the measure the field stars in the stellar neighbourhood of the Milky Way or some extra-galactic system (Scalo, 1986). However, it is difficult to obtain a robust empirical measurement of the IMF in this way because the star-formation history of the Milky Way, or whichever extragalactic system is being used, must be known (Elmegreen and Scalo, 2006). What is actually measured is the present day mass function and, therefore, in order to convert from the observed current distribution to the initial distribution, it must be known how many stars were formed at any given time in the galaxy. Star formation history is poorly understood which means that certain estimations and assumptions have to be made (Bastian et al., 2010). For example, the number of high-mass stars that have gone supernova has to be estimated; assumptions include whether stellar formation was a continuous process or burst like, and whether massive stars form only in massive clusters or also in the field. These estimations and assumptions can can greatly affect the resulting IMF.

Globular clusters are the perfect environment for an in-depth study of the IMF because the shape of the present day stellar mass function of old globular clusters is the combined result of (1) the stellar initial mass function itself; (2) the details of stellar evolution; and (3) dynamical evolution in the Galactic tidal field. All these elements can be modelled in detail (Lamers, 2013), and, in addition, their treatment is greatly simplified because it is safe to assume that dark matter plays a negligible role on their internal dynamics.

1.3 Observations

In 2011, Strader et al. published a paper addressing the stellar mass function of the globular clusters in M31. For convenience, we reproduce Fig. (1) from Strader et al. (2011) showing the mass-to-light ratio of 163 M31 GCs as a function of their metallicity. The points in this plot denote the mass to light ratio of the GCs and the line indicates the trend predicted by a Kroupa IMF that has evolved for 12.5 Gyr. As can be seen, the mass-to-light measurements of these GCs deviate from the model MF prediction, particularly in the case of metal rich GCs. Strader et al. (2011) concluded that these deviations are not caused by standard dynamical evolution and that a shallower mass function for metal rich GCs can explain the observations. The starting point of this project was to question whether the deviations could actually be explained by other means, rather than the conclusion that there must be some sort of metallicity dependent variation in the IMF.

1.4 Plan

The aim of this work was to develop a parameterised model for the present day mass function of GCs that included the effects of stellar evolution and dynamics. This model included the evolution of a population of stars distributed according to a specific IMF, coupled to static dynamics models for GCs with different mass components, such as the multi mass King model. These models were then used to make predictions for the observed velocity dispersion and half light radii which was compared with the observational data of GCs in M31, see Fig. (1).

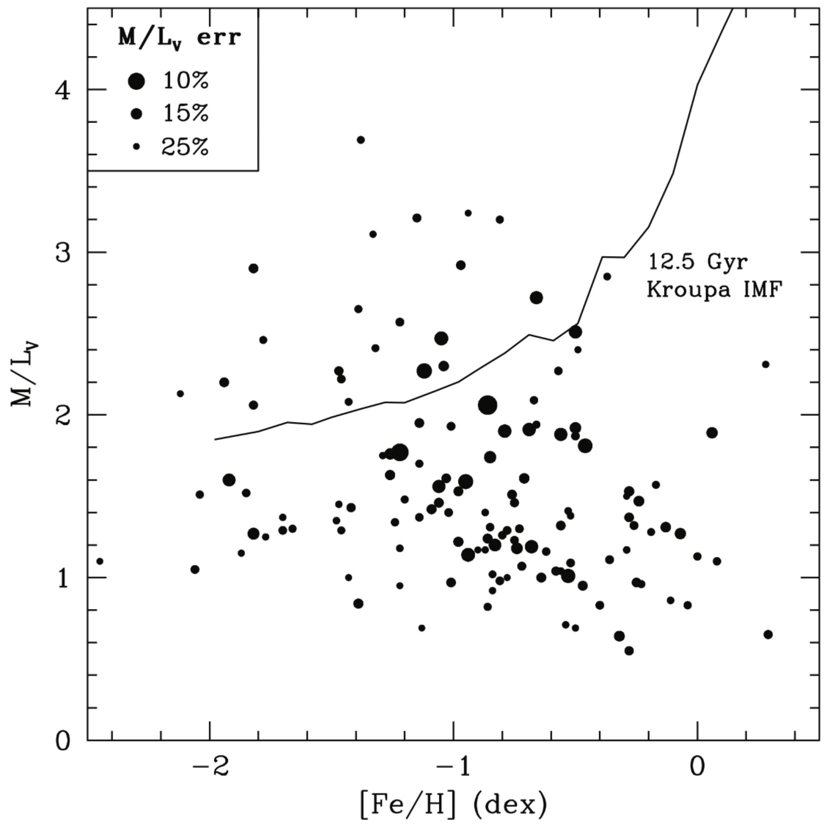

Figure 1: *Taken from Strader et al. (2011). This plot show the mass to light ratio of the 163 GCs from M31, where the size of each point is indicative of its associated error. The line is what you would expect to see for a Kroupa IMF that has evolved for 12.5 Gyr.*

2 Method

2.1 Stellar Evolution

The first step in our analysis was taken by modelling the stellar evolution of 10,000 stars with initial masses ranging between 0.2 and 100 solar masses. We evolved the stars for 12 Gyr using Jarrod Hurley's SSE code (Hurley et al., 2000). We performed this calculation for 11 different metallicities ranging from an [Fe/H] value of -2 to 0. We then used these evolved stars to create an artificial power law stellar mass function for each metallicity:

$$\frac{dN}{dm} = Am^{-\alpha}, \tag{1}$$

where $\alpha = 2.35$. A is a normalisation constant and the total mass is normalised to 1. The benefits of using this synthetic stellar evolution method is that the models can be produced quickly as opposed to having to wait for a full N-body simulation to run. This approach is valid for this work because, for the purpose of our investigation, we do not need to follow the full dynamical evolution of the individual stars but we just need to characterise selected properties of the entire population from a statistical standpoint.

2.2 Dynamics

The second part of our modelling process was focused on the dynamics of the systems. Our approach was based on the use of multi-mass King models, as originally defined by Gunn and Griffin (1979). Such a family of models allowed us to explore the role played by the different mass species, and, in particular, to investigate the retention fraction of "remnant stars" within the star clusters. For a multi-mass model with $N_{\rm bin}$ different mass bins there are $2N_{\rm bin}+1$ parameters: the values of each mass bin accounts for $N_{\rm bin}$ parameters, and the amount of mass in each bin accounts for another $N_{\rm bin}$. The remaining parameter is a fundamental dimensionless parameter, namely the initial concentration, usually denoted by W_0. We wish to emphasise that multi-mass King models define stellar systems in virial equilbrium in which, by definition, the effects of energy equipartition are approximately taken into account, as evident from Fig. (2) (for a full description on the prescription used in the definition of the relationship between the different self-consistent components, see Gunn and Griffin, 1979).

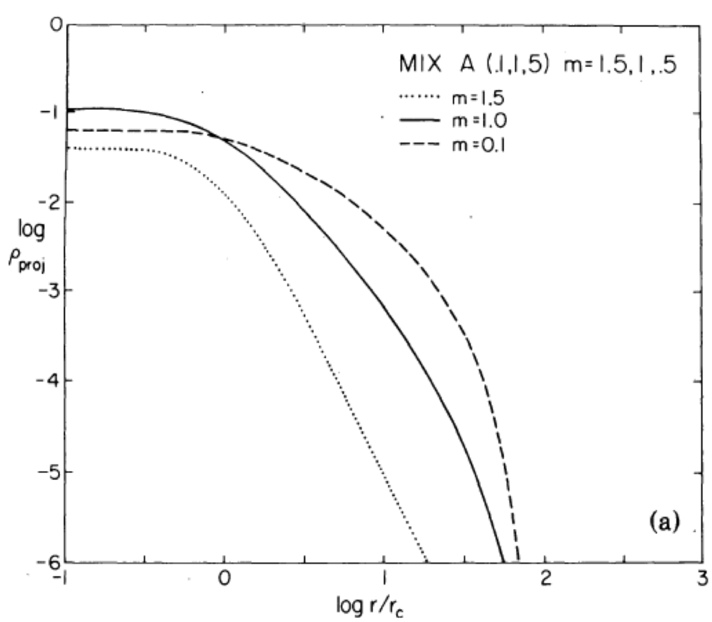

Figure 2: *Multi-mass King model (Gunn and Griffin, 1979). This plot shows the projected surface density as a function of projected radius for three mass species. Mass segregation effects mean that the heavier mass species is more centrally concentrated.*

Fig. (3) shows the density and velocity profiles for the double power law stellar mass function for a metal poor and metal rich cluster. The five mass species are main sequence, evolved stars, white dwarfs, neutron stars and black holes. The mass segregation effect can be seen in the density profiles, whereby the black holes are more centrally concentrated, and therefore, as can be seen in the velocity profiles, they are much slower than the other species.

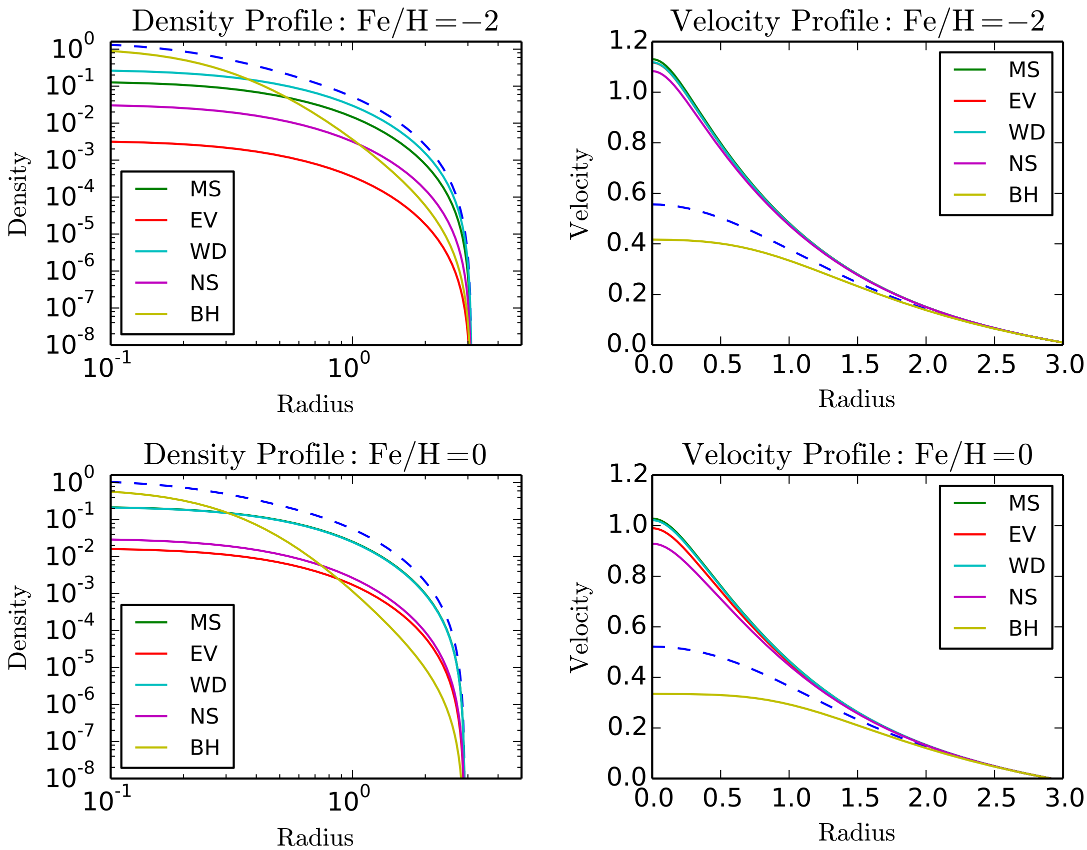

Figure 3: *Density and velocity profiles for a modelled metal poor (top row) GC and a modelled metal rich (bottom row) GC.*

3 Results

3.1 Dynamical to Model Mass Ratio as a function of Metallicity

Starting from the data from Strader et al. (2011) presented in Fig.1, we calculated the values of the ratio between the observed mass and the dynamical mass for each GC in M31, by dividing the mass-to-light ratio of each cluster by its corresponding value on the Kroupa IMF line. As already mentioned, the dynamical models are virial equilibrium configurations and therefore we calculated the value of the observed (i.e. dynamical) mass as $M_{\rm obs} \sim \sigma^2 r_{\rm h}$, and the "true" mass of the model as $M_{\rm mod} \sim 2K/<\sigma^2>$. In the calculation of the relevant structural and dynamical quantities we used exclusively the contribution from the evolved stars, in order to be consistent with the observations.

Fig. (4) shows the observed mass to model mass ratio plotted as a function of metallicity for four different W_0, i.e. central concentration, values. The four W_0 values were chosen to purposefully cover a large parameter space with extreme values in the form of $W_0 = 7$ and $W_0 = 16$.

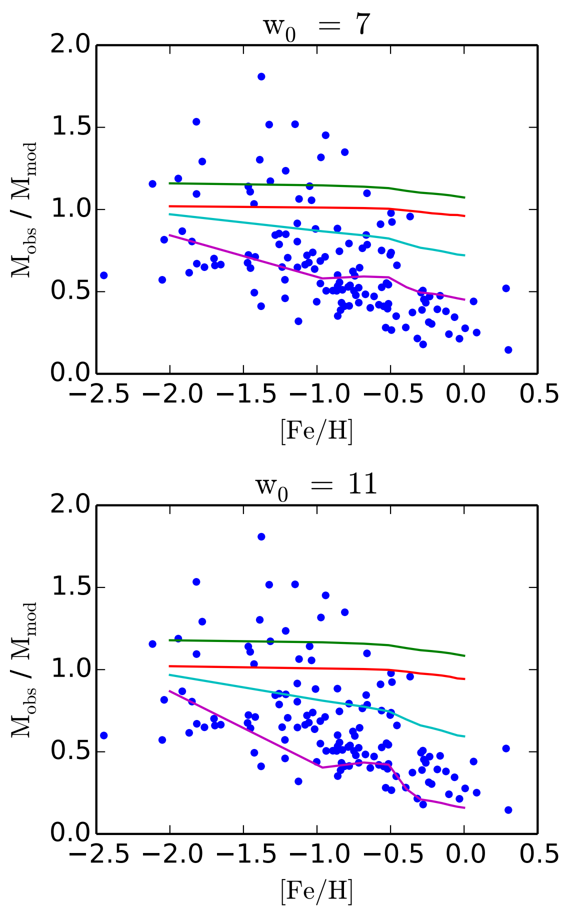

Figure 4: *Observed mass to model mass ratio vs metallicity. Blue points correspond to the data depicted in Fig. (1). The four lines in each plot indicate the different predictions based on different remnant retention fractions: all remanants retained (green),* 10% *of black holes and neutron stars retained (red), no black holes retained (cyan), no neutron stars or black holes retained (purple). Each of the four panels shows the results for King models with different* W_0 *values.*

The four lines in each plot are representative of different remnant retention fractions: all remnants retained, only 10% of both the black holes and neutron stars retained, all of the neutron stars but none of the black holes, and finally none of the neutron stars or black holes retained. These remnant fractions may seem extreme but the actual retention fraction of GCs is still poorly constrained therefore it is important, at this stage, to explore such a large range of possibilities.

The first thing to note from these plots is the surprisingly low $M_{\rm obs}/M_{\rm mod}$ values for many of the GCs, particularly the metal rich ones, which means that the dynamical mass values of the GCs are not representative of the true GC mass. The two extremes of the retention fractions (i.e. all the BH and NS retained and none of the BH and NS retained) encompass the majority of the GC values, especially for $W_0 = 9$ and $W_0 = 11$.

The spacing of the lines shows that the $M_{\rm obs}/M_{\rm mod}$ values of the modelled GCs are incredibly sensitive to the amount of neutron stars and, particularly, black holes retained. This means that when the masses of GCs are measured, unless some offset is included to account for the systematic error arising from the retention fraction, the mass values are not going to be accurate. These results suggest that the offset in Strader's observed GC mass values from the modelled mass values taken from the Kroupa IMF could arise naturally due to the retention fraction of the GCs being unaccounted for, and therefore may not require the mass function itself to be altered.

It can also be seen in Fig. (4) that the $M_{\rm obs}/M_{\rm mod}$ values tend to be larger at lower metallicities, for any given retention fraction. This is because the dynamical mass derived from evolved stars of a mass segregated cluster, i.e. ($M_{\rm obs}$) depends on metallicity, in the sense that $M_{\rm obs}$ is lower, and this effect is stronger at high metallicities. The [Fe/H] dependence is an interesting result that can be explained with some simple stellar evolution argument (Jordán, 2004). The total mass in white dwarfs is higher at low metallicities for the following two stellar evolution effects: (i) the total number of white dwarfs is higher (because the turn-off mass is lower) and (ii) the individual white dwarf masses are higher. This pushes the evolved stars out a bit, and increases their velocities a bit, such that $M_{\rm obs}$ is closer to the actual mass.

3.2 Apparent Concentration as a function of Metallicity

The next step of our analysis was devoted to the inspection of the structural properties of our models, in particular, we examined the ratio of the core radius to half light radius ratio. Once again, we compared the prediction based on our models with the observational data from Strader et al (2011). Fig. (5) shows that for less concentrated models, i.e. $W_0 = 7$, our modelled GCs do not look the same as the Strader GCs which are much less concentrated. However, for increasing W_0 values, the lines cover a more extended area of the parameter space, once again encompassing nearly all the Strader points. If black holes are added, the

$r_0/r_{\rm h}$ values of the evolved stars becomes very large and W_0 must be increased in order to make the $r_0/r_{\rm h}$ value of the evolved stars within the range of the observations. Interestingly, increasing W_0 does not affect the ratio $M_{\rm obvs}/M_{\rm mod}$ too much.

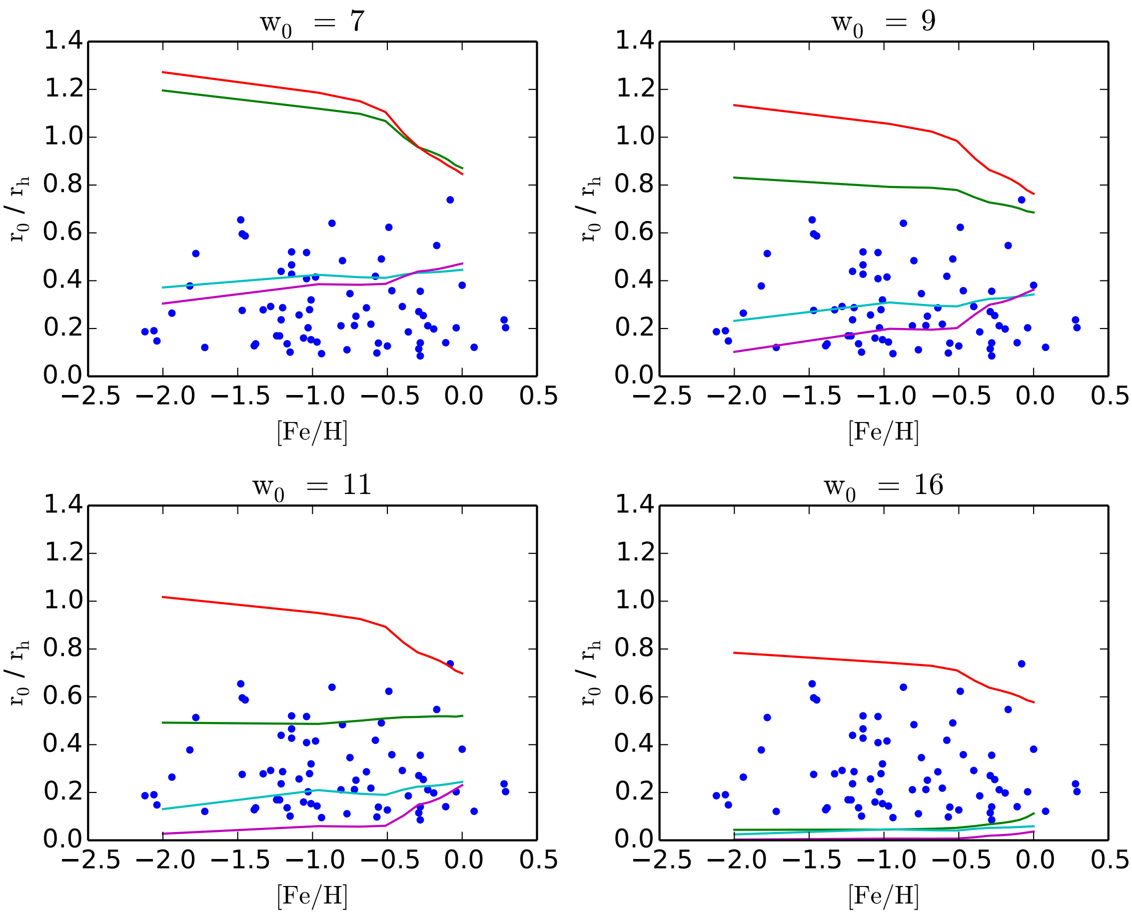

Figure 5: *Core radius to half light radius ratio vs metallicity. The four panels, and the colours of the lines and points correspond to those in Fig. (4).*

3.3 Apparent Concentration as a function of Dynamical to Model Mass Ratio

Finally, we explored the plane ($M_{\rm obs}/M_{\rm mod}$, r_0/rh) for three selected values of metallicity (see Fig. (6)). Also in this case, the range of the values covered by the prediction based on our models, especially those in the regime of high concentration, is quite consistent with the observational data from Strader et al (2011). This result is in agreement with the findings described in the previous sections.

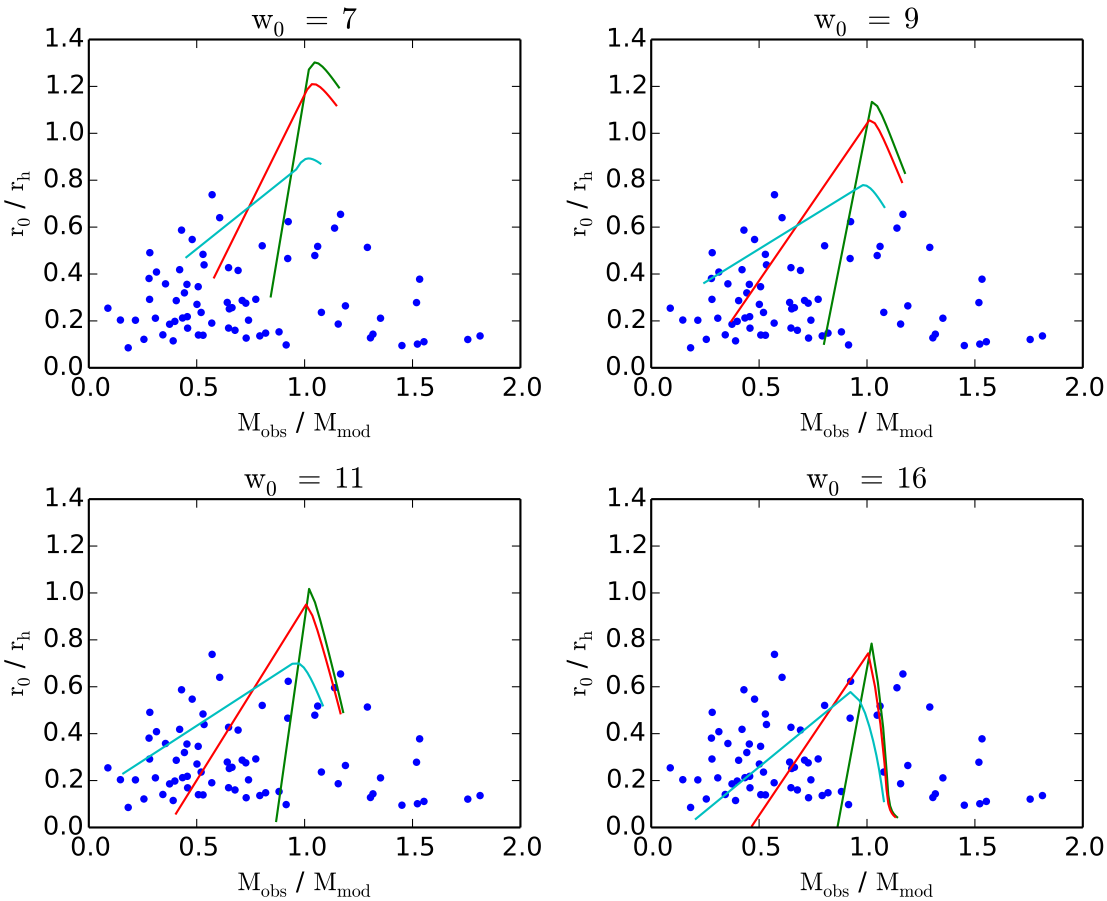

Figure 6: *Core radius to half light radius ratio vs observed mass to model mass ratio. The blue points once again correspond to the results from Fig. (1), the lines show different [Fe/H] values: -2 (green), -1 (red), 0 (cyan).*

3.4 Key Results

- For clusters without neutron stars and without black holes, the dynamical mass derived from evolved stars of a mass segregated cluster depends on metallicity, in that $M_{\rm obs}$ is lower, and this effect is stronger at high metallicities.
- Adding blackholes has a large effect on the derived $M_{\rm obs}$, in that the value is higher, and closer to the real value. Neutron stars also increase the derived $M_{\rm obs}$ but not by as much.

4 Summary

This work has been a preliminary investigation. Our goal was to explore alternative explanations to the measured deviations from the IMF of the M31 GCs. We did this by using a somewhat crude stellar mass function model and explored the effect of using different central concentration values, metallicities, and remnant retention fractions. We found that the amount of remnants within the GC dramatically alters the measured dynamical mass compared to the actual mass of the GC and that this could go some way to explaining the discrepancy as highlighted by Strader et al. (2011). Whilst these results are preliminary, they are already indicating some very interesting physical effects that warrant further investigation. We will next look to expand our investigation by more including different retention fractions, and a more elegant stellar mass function, in the hope that we can further explain the observations of GCs. In conclusion, the exploration of the effects of a more realistic dynamical modelling approach seems to be a very promising route to understand the physical origin of the surprising properties of the mass-to-light ratios of the star clusters in M31.

5 References

Bastian, N., Covey, K. R., and Meyer, M. R. (2010) *ARA&A*, **48**, 339.
Elmegreen, B. G. and Scalo, J. (2006) *ApJ*, **636**, 149.
Gunn, J. E. and Griffin, R. F. (1979) *AJ*, **84**, 752.
Hurley, J. R., Pols, O. R., and Tout, C. A. (2000) *MNRAS*, **315**, 543.
Jordán, A. (2004) *ApJ*, **613**, L117.
Lamers, H., Baumgardt, H., and Gieles, M. (2013) *MNRAS*, **433**, 1378.
Scalo, J. M. (1986) *FCPH*, **11**, 1.
Strader, J., and Caldwell, N., and Seth, A. C. (2011) *AJ*, **142**, 8.